THE JOURNAL OF PHYSICAL CHEMISTRY C

ARTICLE

pubs.acs.org/JPCC

Effect of Al_2O_3 Nanoparticles on Radiolytic H_2O_2 Production in Water

Olivia Roth,[†] Akihiro Hiroki,[§] and Jay A. LaVerne*[,†,‡]

[†]Radiation Laboratory and [‡]Department of Physics, University of Notre Dame, Notre Dame, Indiana 46556, United States

[§]Environmental Radiation Processing Group, Quantum Beam Science Directorate, Japan Atomic Energy Agency, Takasaki, Gunma 370-1292, Japan

ABSTRACT: The yields of H_2O_2 have been determined in aqueous slurries in the pH range of 1−13 with various amounts of added Al_2O_3 nanoparticles. The addition of Al_2O_3 generally decreases H_2O_2 yields at all pH values within this range in the gamma radiolysis of both deaerated and aerated slurries, except at pH above 11. Very little effect of pH is observed in the gamma radiolysis of deaerated systems in the pH range of 3−8, whereas a large increase in H_2O_2 yields is observed in aerated Al_2O_3 slurries as the pH increases or decreases from neutral. Results with 5 MeV H and He ions for H_2O_2 yields in aerated Al_2O_3 slurries above pH 4 have similar trends as in gamma radiolysis, except with different absolute yields. Scavenger capacity studies using methanol as an $OH^•$ radical scavenger show that the decrease in H_2O_2 yields with added Al_2O_3 occurs at relatively long time scales and is probably due to reaction of the solid nanoparticles with $OH^•$ radicals.

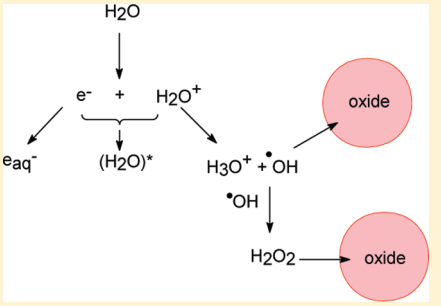

INTRODUCTION

Many issues remain unresolved on the behavior of hydrogen peroxide, H_2O_2, in the radiolysis of complex systems involving water and metal oxide surfaces. Hydrogen peroxide is one of the main oxidizing products formed in the radiolysis of water, and its chemistry is extremely important throughout the nuclear industry such as in the operation of nuclear reactors[1] and in the storage of spent nuclear fuel.[2] The radiolysis of systems containing water and metal oxide surfaces is also of fundamental importance because of the possible transport of energy, charge, or species through the interface, thereby affecting product formation as compared to the radiolysis of the individual components.[3,4]

The mechanism for H_2O_2 formation and its radiation chemical yield are well-known in dilute aqueous solutions.[5,6] Previous studies have shown that the radiation chemical yield of H_2 from water can be significantly altered by the presence of ceramic oxides,[3,4] and it is reasonable to believe that the radiolytic production of H_2O_2 from water is also affected by solid interfaces. All radiolysis products of water (e_{aq}^-, $H^•$, $OH^•$, $HO_2^•$, H_2O_2, and H_2) are connected through a complex scheme of reactions.[7,8] Hence, the interactions between all water decomposition species with the solid surface could potentially be important to resolve the evolution of a single radiolysis product.

Adsorption and catalytic decomposition of H_2O_2 on various solid surfaces has been studied extensively.[9−16] Radical species can be stabilized on solid surfaces, and their lifetime, and thereby reaction scheme, can be altered.[15] No study has so far been put forward examining the combined effects of these processes on the production of H_2O_2 during the radiolysis of water in contact with solid surfaces. This study focuses on the effect of aluminum oxide, Al_2O_3, on the radiolysis of liquid water. Aluminum has an oxide surface, and its alloys can be found as construction and cladding materials in nuclear reactors.[3,17]

The radiation chemical yield of H_2O_2 has been measured in this work as a function of pH in the range of 1.3−12.5 in the gamma radiolysis of slurries consisting of nanometer-sized Al_2O_3 particles and an aqueous phase of either 25 mM $NaNO_3$ (argon-saturated) or air-saturated water (0.25 mM O_2). Effects due to variation in the scavenging capacity for $OH^•$ radicals and hydrated electrons, e_{aq}^-, in the gamma radiolysis of Al_2O_3 slurries were studied at neutral pH using varying concentrations of methanol and $NaNO_3$, respectively. Irradiations were also performed using 5 MeV ^1H and ^4He ions to mimic the response expected for the recoils of neutrons and alpha particles, respectively. The heavy ion results are compared with the results of gamma radiolysis to show the chemical effects due to track structure. The influence of Al_2O_3 on the mechanisms for the formation and reaction of H_2O_2 in the radiolysis of water and aqueous solutions is discussed.

EXPERIMENTAL SECTION

Irradiations. Irradiations with γ rays were performed using a self-contained Shepherd 109-68 cobalt-60 source at the Radiation Laboratory of the University of Notre Dame. Sample cells were Pyrex tubes 10 mm in diameter and about 10 cm long. Samples were degassed with ultra high purity argon or left aerated and then flame-sealed. The dose rate was 57.8 Gy/min as determined using the Fricke dosimeter. Samples were irradiated at room temperature to a total dose of 462 Gy. Samples were continuously mixed vertically by rotating the sample cells during irradiation.

Received: December 15, 2010
Revised: February 21, 2011
Published: March 31, 2011

Heavy ion irradiations were performed in continuously purged and vigorously stirred cells using the Tandem FN Van de Graaff facility of the Notre Dame Science Laboratory in the University of Notre Dame Physics Department. The ions used in these experiments were 5 MeV $^1H^+$ and 5 MeV $^4He^{2+}$. These energies were incident to the sample with energy loss to windows determined using standard stopping power compilations.[18] Irradiation methods and ion characteristics have been described previously.[1,7] Absolute dosimetry techniques were used by combining ion energy with integrated beam currents. Ion beam currents were typically 1.5 nA charge, and doses up to 1200 Gy were used.

Materials. Chemicals of the highest grade available were used as received without further purification. Water was 10^{18} Ω-cm as obtained from the Radiation Laboratory in house H2Only system, which consists of UV lamps and multiple filters. Argon used for purging was of ultrahigh purity. The Al_2O_3 particle surface area was determined to be 8.09 m^2/g, using the BET (Brunauer−Emmet−Teller) method and a Quantachrome Autosorb 1 analyzer. This area corresponds to a perfect sphere of about 185 nm. The Al_2O_3 was baked at 500 °C for 48 h prior to the experiment to remove any hydrocarbon contaminants.

Radiolytic H_2O_2 yields were determined as a function of pH using samples consisting of 0.5−1.0 g of Al_2O_3 (Alfa Aesar) and 3 mL of aqueous phase. The aqueous phase was either 25 mM $NaNO_3$ (Aldrich) argon-saturated solution or air-saturated water. The decomposition of H_2O_2 on Al_2O_3 was studied as a function of pH in 60 μM H_2O_2 solutions containing 1.0 g of Al_2O_3 per 3 mL of aqueous solution. The pH of the solutions was varied from 1.3 to 12.5 by the addition of H_2SO_4 (Fischer Scientific) or KOH (Fischer Scientific). The pH of the samples was determined prior to irradiation using an Orion 420A pH meter.

Scavenging capacity effects on $OH^•$ radicals and e_{aq}^- were examined in the radiolysis of 1.0 g of Al_2O_3 in 3 mL of solution. The aqueous phases were either argon-saturated solutions containing 25 mM $NaNO_3$ and 10 μM to 10 M methanol (Sigma-Aldrich) or argon-saturated solutions containing 0.25 mM to 8 M $NaNO_3$.

Analysis. The samples were filtered (minimum 0.45 μm) and analyzed immediately after irradiation. Concentrations of H_2O_2 were measured using the Ghormley method,[19,20] which is based on the oxidation of I^- to I_3^- by H_2O_2 and the spectrophotometrical determination of I_3^- at 350 nm. The reaction between H_2O_2 and I^- was carried out in slightly acidic solutions buffered with 100 mM phthalic acid/phthalate (Aldrich) or 1 M acetic acid/acetate (Sigma-Aldrich) depending on the pH of the sample. Samples of 2 mL of irradiated solution were added to 1 mL of buffer solution and 1 mL of reagent solution containing 0.4 M KI (Sigma-Aldrich) and 160 μM $(NH_4)_6Mo_7O_{24}$ (Aldrich). Changes in the absorbance of the solutions were measured using a diode array spectrophotometer (Hewlett-Packard HP8453). The extinction coefficient was 24135 M^{-1} cm^{-1}, which is consistent with previous studies.[1,5]

RESULTS AND DISCUSSION

A number of parameters will have an effect on the measured yield of H_2O_2 in the studied systems. These effects range from the interaction of water radiolysis products with H_2O_2 to catalytic decomposition of the H_2O_2 by the oxide interface. Selected scavengers can be used to mitigate radiolysis effects, but these systems always have measured yields that are different than the primary H_2O_2 yields. Some of the radiation chemical effects of pH on H_2O_2 yields have already been examined in aqueous solutions without added oxides.[21]

When exposed to ionizing radiation, water decomposes within a few picoseconds of the energy deposition to give e_{aq}^-, $H^•$, $OH^•$, $HO_2^•$, and H_2.[6] These species are located in spurs along the path of the incident γ radiation or within the columnar structure of the heavy ion tracks.[22] Outward diffusion of these species competes with their reactions with each other, and within a few microseconds following the energy deposition, the species are nearly homogeneously distributed. The chemistry occurring within the track or spur can be described by ten main radical reactions.[23] Of these reactions, H_2O_2 is almost exclusively formed on the submicrosecond time scale by the combination of $OH^•$ radicals.[5]

$$OH^• + OH^• \rightarrow H_2O_2 \quad k = 5.5 \times 10^9\ dm^3\ mol^{-1}\ s^{-1} \quad (1)$$

Rate constants used throughout the manuscript are from Buxton et al.[24] unless otherwise stated. Reaction 1 competes in the spur or track with the reaction of $OH^•$ radicals with $H^•$ atoms and e_{aq}^-, reactions 2 and 3.

$$e_{aq}^- + OH^• \rightarrow OH^- \quad k = 3.0 \times 10^{10}\ dm^3\ mol^{-1}\ s^{-1} \quad (2)$$

$$H^• + OH^• \rightarrow H_2O \quad k = 7.0 \times 10^9\ dm^3\ mol^{-1}\ s^{-1} \quad (3)$$

Radicals that escape reactions within the track may react with H_2O_2 in the homogeneous phase to reduce its long-term concentration and thereby alter the measured yield. For this reason, radical scavengers must be added to the solutions when measuring H_2O_2 yields.[21]

The catalytic decomposition of H_2O_2 on the oxide surface must be considered in the long-term evolution of the H_2O_2 concentration. Metal ions in their reduced states are well-known to catalyze H_2O_2 decomposition through the Fenton reaction.[25] H_2O_2 is also decomposed on metal oxides where the cations are in their highest oxidation state. Although these reactions have been studied extensively, the mechanisms are not completely elucidated. In particular, the role of $OH^•$ radicals has been subject to debate.[26,27] A recent study has found that the dynamics of $OH^•$ radical formation during H_2O_2 decomposition on ZrO_2 is consistent with a mechanism involving the $OH^•$ radical as well as the $HO_2^•$ radical.[28] The involvement of radical intermediates adsorbed on the solid surface has also been proven by EPR studies.[15] These later studies have found $O_2^{•-}$, $O^{•-}$, and $OH^•$ radicals to be stabilized in magnesium oxide following its exposure to H_2O_2. Similar species may be expected to form on Al_2O_3 exposed to H_2O_2.

Adsorption of species on a solid surface will be strongly affected by the pH of the solution. Changes in pH of the solutions lead to protonation or deprotonation of the water molecules or OH groups adsorbed on the solid interface. At high pH the surface will be negatively charged, and adsorption of cations is facilitated; however, negatively charged ions will be attracted at low pH. Maximum adsorption of neutral molecules will occur at the pH at which the surface exhibits no net charge and the competition for adsorption sites is minimized.[29,30] This value of the pH is referred to as the point of zero charge, PZC.

As the catalytic decomposition of H_2O_2 on a solid surface is preceded by surface adsorption, the rate of decomposition is expected to be dependent on the surface charge. A study by Wright and Rideal[30] shows a correlation between the maximum rate of H_2O_2 decomposition and the minimum surface charge. Lousada and Jonsson[28] have found that the rate constant for H_2O_2 decomposition increases linearly with increasing pH in the range of pH from 2−11. The authors attribute this effect to a combination of formation of stable H_2O_2 clusters on the surface

Table 1. Pseudo First-Order Rate Constant for H_2O_2 Decomposition on Al_2O_3[a]

pH	k (s^{-1})
1	0.0023
3	0.0057
7	0.0198
10	0.0299

[a] Error is 5%.

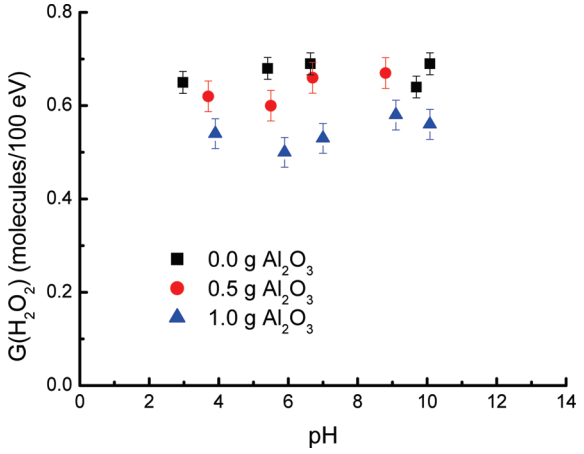

Figure 1. Gamma radiolysis H_2O_2 yields as a function of pH for different amounts of Al_2O_3 in 3 mL of 25 mM NO_3^- aqueous solutions, corrected for catalytic decomposition of H_2O_2 on Al_2O_3: (■) no Al_2O_3, (●) 0.5 g of Al_2O_3, (▲) 1.0 g of Al_2O_3.

at low pH and the competition with the superoxide radical for available surface sites.

The natural decay rate of H_2O_2 in the presence of Al_2O_3 must be determined to distinguish catalytic effects at the particle surface from radiolysis effects. The pseudo first-order rate constant for decomposition of H_2O_2 on Al_2O_3 has been determined using 60 μM H_2O_2 solutions containing 1.0 g Al_2O_3 per 3 mL of aqueous solution. Concentrations of H_2O_2 were determined at various delay times following the mixing of the solution and Al_2O_3. The rate constants given in Table 1 are obtained from the observed decrease in H_2O_2 concentrations and are found to increase linearly with pH in the range 1−10. At pH 13, relatively slow HO_2^- decomposition is observed initially, and the decomposition stops when ~40% of the peroxide has been consumed, indicating saturation of the surface. Since no product analysis was performed, it is not possible to distinguish between H_2O_2 decomposition and adsorption in the present experiment. Corrections to measure radiation chemical yields due to the catalytic decomposition of H_2O_2 obviously depend on the irradiation time but were typically on the order of a few percent.

The measured H_2O_2 yields in the gamma radiolysis of 25 mM NO_3^- solutions are shown in Figure 1 as a function of pH in the range of 3−10 in the presence and absence of Al_2O_3. Outside this range, the H_2O_2 yield will be strongly reduced by secondary reactions of the NO_3^- at both lower and higher values of pH as described by Roth and LaVerne.[21] The NO_3^- anion is used to scavenge e_{aq}^- to minimize decomposition of H_2O_2 by this species. As can be seen in the figure, the measured H_2O_2 yield decreases with an increasing amount of added Al_2O_3. This decrease cannot be due to catalytic decomposition of the H_2O_2 as this process amounts to only a few percent and is subtracted from the measured radiolytic yield. The observed decrease in H_2O_2 yield is most likely due to interactions between radical radiolysis products and the solid surface. As mentioned above, sorption of radical species could influence the radiolytic yield of H_2O_2 by changing the lifetime and reaction scheme of, for example, H_2O_2 precursors such as the $OH^\bullet$ radical. Giamello et al. found that interfacial reactions of liquid-phase H_2O_2 with magnesium oxide resulted in $OH^\bullet$ radicals trapped in the matrix with high thermal stability.[15] Actually two related phenomena may be occurring to reduce the yield of H_2O_2 in the presence of the Al_2O_3. The oxide surface may be trapping $OH^\bullet$ radicals and thereby decreasing the production of H_2O_2, and the stabilized $OH^\bullet$ radicals may live long enough to react with H_2O_2. Although Giamello et al. claim the $OH^\bullet$ radicals are trapped in the matrix, they must still be at or near the surface and may undergo reaction. $OH^\bullet$ radicals readily react with H_2O_2, but they normally disappear quickly in the radiolysis of water. Stabilization of $OH^\bullet$ radicals with H_2O_2 on the oxide surface could increase the decomposition of H_2O_2 as well as lower its formation through reaction 1.

Table 2. Values of pK_a for the Radiolysis Products of Water

	pK_a
$HO_2^\bullet \leftrightarrows O_2^{\bullet-} + H^+$	4.57
$H^\bullet \leftrightarrows e_{aq}^- + H^+$	9.77
$H_2O_2 \leftrightarrows HO_2^- + H^+$	11.65
$OH^\bullet \leftrightarrows O^{\bullet-} + H^+$	11.9

As can be seen in Figure 1, the yield of H_2O_2 is not very dependent on pH in the studied range. When exploring the pH effects on the decomposition and formation of H_2O_2, not only surface charge but also the pK_a of involved species in solution have to be taken into account. The pK_a values of the relevant species in water radiolysis are presented in Table 2. The only radiolysis species with values of pK_a in the studied range is $HO_2^\bullet$ (pK_a 4.57). This species has a very low yield in deaerated solution, and it is not expected to influence the chemistry significantly. The PZC for Al_2O_3 is around 8.5.[31] No significant change in the magnitude of the effect is observed at this pH, indicating that no charged species are involved in the surface reaction.

Aerated solutions were used to measure H_2O_2 throughout the pH range, which allows further investigation of pH and surface charge effects. The presence of oxygen will increase the production of H_2O_2 through the formation and recombination of $HO_2^\bullet/O_2^{\bullet-}$ (reactions 4−8).

$$O_2 + e_{aq}^- \rightarrow O_2^{\bullet-} \quad k = 1.9 \times 10^{10}\ dm^3\ mol^{-1}\ s^{-1} \quad (4)$$

$$O_2 + H^\bullet \rightarrow HO_2^\bullet \quad k = 2.1 \times 10^{10}\ dm^3\ mol^{-1}\ s^{-1} \quad (5)$$

$$HO_2^\bullet + HO_2^\bullet \rightarrow H_2O_2 + O_2 \quad k = 7.0 \times 10^5\ dm^3\ mol^{-1}\ s^{-1} \quad (6)^8$$

$$HO_2^\bullet + O_2^{\bullet-} \rightarrow HO_2^- + O_2 \quad k = 8.0 \times 10^7\ dm^3\ mol^{-1}\ s^{-1} \quad (7)^8$$

$$O_2^{\bullet-} + O_2^{\bullet-} + 2H_2O \rightarrow H_2O_2 + O_2 + 2OH^- \quad k = 1 \times 10^2/[H_2O]^2\ dm^9\ mol^{-3}\ s^{-1} \quad (8)^8$$

In Figure 2, the measured H_2O_2 yields in gamma-irradiated aerated systems with and without Al_2O_3 are shown. As can be seen, the H_2O_2 yield is reduced by the presence of Al_2O_3

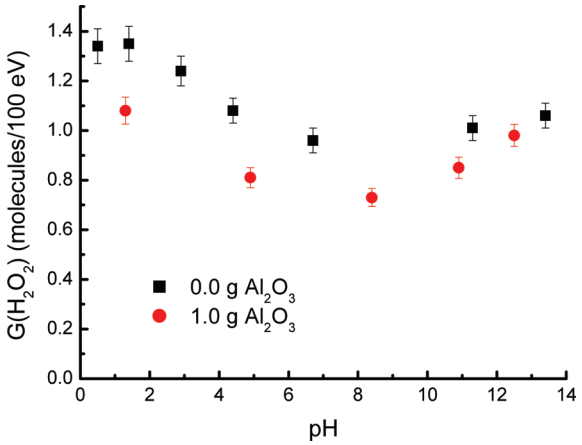

Figure 2. H_2O_2 yields as a function of pH in the gamma radiolysis of 3 mL of aerated water, corrected for catalytic decomposition of H_2O_2 on Al_2O_3: (■) no Al_2O_3, (●) 1.0 g of Al_2O_3.

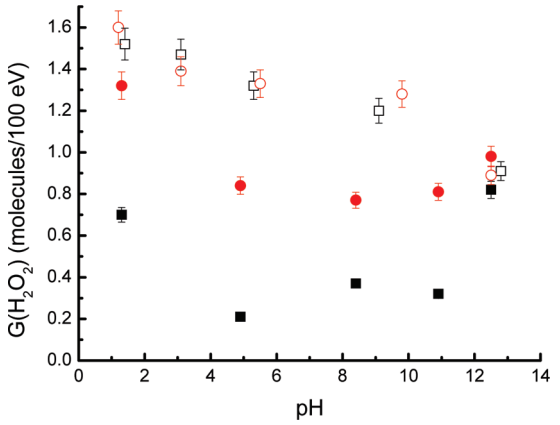

Figure 3. H_2O_2 yields as a function of pH in the ^1H and ^4He ion radiolysis of 3 mL of aerated water, corrected for catalytic decomposition of H_2O_2 on Al_2O_3: (□) ^1H no Al_2O_3, (■) ^1H 1.0 g of Al_2O_3, (○) ^4He no Al_2O_3, (●) ^4He 1.0 g Al_2O_3.

throughout the studied pH range, except at values of pH greater than 11. The magnitude of the observed decrease at neutral and slightly alkaline pH is similar to the observations in the nitrate systems and can probably be explained by the same mechanism. Under highly alkaline conditions, the observed results can probably be attributed to the deprotonation of $OH^•$ radicals (pK_a 11.9). The deprotonated $O^{•-}$ species is repelled by the negatively charged surface that is formed above about pH 8.5, and the adsorption of the radical is decreased thereby decreasing the influence of the surface on the H_2O_2 production. The result is that most of the chemistry is occurring in the aqueous phase, and the presence of the oxide is not important.

With decreasing pH the e_{aq}^- is converted to $H^•$ atoms at shorter times. The reaction of the $H^•$ atom with H_2O_2 is about 2 orders of magnitude slower than that of the e_{aq}^-, resulting in a slight protective effect on H_2O_2. The result is an increase in H_2O_2 yield with decreasing pH. A pronounced effect of added Al_2O_3 on H_2O_2 yields is observed in aerated slurries at lower values of pH. In contrast to the nitrate system, the $HO_2^•$ radical will play a major role in the H_2O_2 evolution in aerated solutions. In the presence of oxygen, a large portion of the H_2O_2 is produced by the combination of $HO_2^•/O_2^{•-}$ radicals (reactions 6−8). $HO_2^•$ is a week acid (pK_a 4.57) and can also easily deprotonate in the presence of metal oxide surfaces according to reaction 9.[13]

$$HO_2^• \rightarrow H^+ + O_2^{•-} \quad (9)$$

The formed $O_2^{•-}$ radical is adsorbed and stabilized on the oxide surface. Decreasing the pH could increase the stabilization of superoxide on the surface. This increased stability could potentially decrease the impact of reactions 6−8 and account for the slightly larger effect of the added oxide at low pH values.

For comparison with gamma radiolysis, the aerated system was also studied with radiolysis by 5 MeV $^1H^+$ and 5 MeV $^4He^{2+}$ with results shown in Figure 3. The heavier ions have an increased linear energy transfer (LET = stopping power, $-dE/dx$) resulting in an increased extent of second-order reactions, which should lead to an increase in H_2O_2 yields due to enhanced combination reactions of $OH^•$ radicals, reaction 1, within the track of the incident ion.[1] On the other hand, increasing LET results in a decrease in e_{aq}^- and $H^•$ atom yields that escape the ion track. These two radical species would normally react with O_2, so the result is a decrease in $HO_2^•/O_2^{•-}$ radical yields in aerated slurries with increasing LET. Combination reactions of the $HO_2^•/O_2^{•-}$ species lead to a significant fraction of the H_2O_2 formed in aerated solutions.[21] The near similarity of yields for both H and He ions without added oxide suggests that the increase in LET for He ions leads to an increase in the intratrack production of H_2O_2 that is nearly the same as the amount of H_2O_2 not produced because of a slight decrease in radicals escaping the track. Yields of H_2O_2 are nearly the same for γ rays, H ions, and helium ions at pH 1 and 14 without added oxide. Slight differences are observed between the results for γ rays and for H/He ions at intermediate pH values, which is probably due to the changing contributions of intratrack and homogeneous reactions in the production of H_2O_2.

As can be seen in Figure 3, the H_2O_2 yield in the slurries is approximately constant in the range of pH ∼4−11, whereas higher yields are observed at pH outside of this range. The observed H_2O_2 yields with Al_2O_3 are significantly lower than the yields in systems without oxide, except at pH less than 4 or greater than 11. At pH greater than 11, the effect of added oxide is negligible for γ rays, H ions, and He ions. As discussed above, this result is due to the surface repulsion of the $O^{•-}$ formed by the dissociated $OH^•$ radical. Most of the chemistry is then occurring in the water phase alone.

In the gamma-irradiated system, the addition of the oxide was observed to lower H_2O_2 yields at pH below 11. The effect of added oxide is more pronounced with high LET radiation in the mid range of pH. In the radiolysis with He ions at neutral pH, the H_2O_2 yield with added Al_2O_3 is only two-thirds of that for aqueous solutions alone, and even lower yields are observed with H ions. The difference in H_2O_2 yields between H ions and He ions is due to the decrease in $HO_2^•/O_2^{•-}$ radical yields with increasing LET. More of the H_2O_2 produced in the radiolysis with H ions is due to long time reactions of $HO_2^•/O_2^{•-}$ radicals. These species or their precursors react with the added Al_2O_3 to reduce the production of H_2O_2 in the mid pH range. The mechanism for H_2O_2 reduction is then the same as discussed above with γ rays.

To probe the time scale of the processes involved in the interactions between the solid surface and products of water radiolysis, the H_2O_2 yield in gamma-irradiated Al_2O_3 slurries was studied as a function of $OH^•$ radical scavenging capacity. The method of varying the $OH^•$ radical scavenging capacity to probe

dx.doi.org/10.1021/jp111918v |J. Phys. Chem. C 2011, 115, 8144–8149

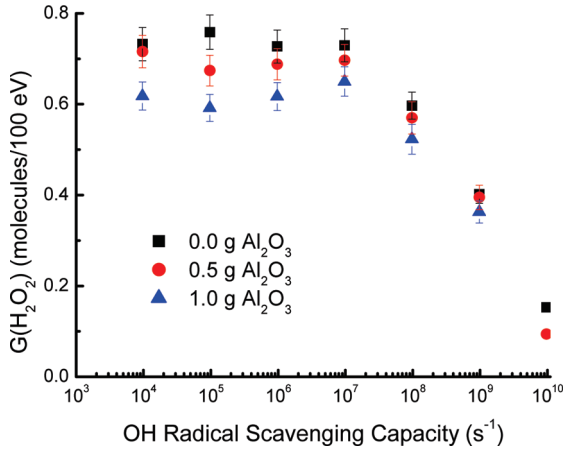

Figure 4. Gamma radiolysis H_2O_2 yields at neutral pH as a function of OH scavenging capacity with methanol for different amounts of Al_2O_3 in 3 mL of aqueous solutions of 25 mM NO_3^-, corrected for catalytic decomposition of H_2O_2 on Al_2O_3 taking the effect of methanol into account: (■) no Al_2O_3, (●) 0.5 g of Al_2O_3, (▲) 1.0 g of Al_2O_3.

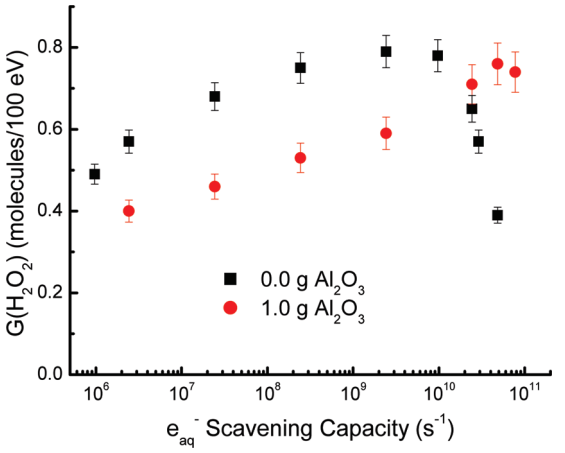

Figure 5. Gamma radiolysis H_2O_2 yields at neutral pH as a function of hydrated electron scavenging capacity with NO_3^- for different amounts of Al_2O_3 in 3 mL of solution corrected for catalytic decomposition of H_2O_2 on Al_2O_3: (■) no Al_2O_3, ref 5, (●) 1.0 g of Al_2O_3.

the temporal dependence of the formation of H_2O_2 has been used and described previously.[1,5] The lifetime of the radical with respect to the scavenger is approximately equal to the inverse of the scavenging capacity. In Figure 4 the H_2O_2 yield is shown as a function of $OH^•$ radical scavenging capacity using methanol as the scavenger. As described by Pastina and LaVerne,[1] the limiting value at low scavenging capacity corresponds to the escape yield of H_2O_2, while the higher $OH^•$ radical scavenging capacities correspond to the time-dependent evolution of the spur.

At about 10 ns scavenging capacity of 10^8 s^{-1}, the effect of added Al_2O_3 on H_2O_2 yields becomes noticeable. The results suggest that H_2O_2 formation at short times, <10 ns, is dominated by the water chemistry alone, whereas the effect of added oxide is on a relatively long time scale. The escape yield is reached around 0.1 μs. Addition of the oxide results in the loss of H_2O_2 by scavenging its precursor, the $OH^•$ radical, which would occur on relatively long times as the $OH^•$ radical diffuses to the Al_2O_3 surface. Also, the trapped $OH^•$ radicals could further react with H_2O_2 on long time scales as it also diffuses to the oxide surface. Previous studies have shown that methanol strongly affects the decomposition of H_2O_2 on Al_2O_3.[27] Catalytic decomposition of the H_2O_2 has been taken into account by subtraction of the expected decomposition under similar conditions without radiolysis.

The H_2O_2 yield as a function of e_{aq}^- scavenging capacity was studied in aqueous solutions by Hiroki and LaVerne using NO_3^- as the scavenger and is shown in Figure 5.[27] They found that the H_2O_2 yield increases with increasing scavenging capacity up to 2.9×10^9 s^{-1}, followed by a decrease at even higher scavenging capacities. The initial increase can be explained by the scavenging of e_{aq}^- preventing its reaction with $OH^•$ radicals through reaction 2, thereby leaving more $OH^•$ radicals available for H_2O_2 production. Scavenging of the e_{aq}^- also limits its direct reaction with and decomposition of H_2O_2. In the heterogeneous system shown in Figure 5, the H_2O_2 yield increases with increasing e_{aq}^- scavenging capacity throughout the range of NO_3^- concentrations used in this work. The decrease in H_2O_2 production observed in the aqueous system at very high scavenging capacities is not observed in the presence of the Al_2O_3.

The yield of H_2O_2 in water alone should reach a limiting value with increasing e_{aq}^- scavenging capacity. A reasonably constant value of 0.78 molecules/100 eV is observed at a scavenging capacity of 10^{10} s^{-1}. The results with added Al_2O_3 are observed to approach a similar value at high scavenging capacity suggesting that the oxide has little effect on the H_2O_2 chemistry at short times. The sharp drop off in H_2O_2 yields for water without Al_2O_3 at scavenging capacity greater than 10^{10} s^{-1} was originally attributed to NO_3^- scavenging of the $H_2O^{•+}$ water cation, which is the direct precursor to $OH^•$ radicals.[5] No decrease in H_2O_2 yields are observed at high scavenging capacity with added Al_2O_3, suggesting that the solid surface prevents the scavenging of the OH radical precursor. The equivalent concentration of 1 g of Al_2O_3 in 3 mL is about 3 M if the oxide is soluble. Such a high concentration of a solute could react with the very short-lived water cations if the rate constant for such a reaction was extremely high. However, with Al_2O_3 powders the density of surface sites is low, and there is no special reason for this material to be very reactive with water cations. There is no obvious reason why the added Al_2O_3 should have a significant effect on such short time chemistry. Another possibility for the decreased H_2O_2 yield at high scavenging capacity could be due to secondary reactions of a product from the e_{aq}^- reaction with NO_3^- that is reactive with H_2O_2 leading to a reduction in the observed yield of H_2O_2. Reaction of this product with the H_2O_2 could occur at much longer times, so high concentrations of this product would not be required to have an observable effect. However, there is still no explanation why the same process does not occur in the presence of Al_2O_3 unless the oxide surface somehow traps or reacts with the product before it can decompose the H_2O_2.

■ CONCLUSIONS

The yields of H_2O_2 have been determined in aqueous slurries in the pH range of 1−13 with various amounts of added Al_2O_3 nanoparticles. Gamma radiolysis of deaerated solutions show very little variation in H_2O_2 yields with pH in the range of 3−8, but the addition of Al_2O_3 decreases H_2O_2 yields at all pH values. Gamma radiolysis of aerated solutions shows an increase in H_2O_2 yields as the pH increases or decreases from neutral, and again the addition of Al_2O_3 decreases the H_2O_2 yield, except at pH above 11. Both the 5 MeV H ion and the 5 MeV He ion radiolysis of aerated slurries result in a decrease in H_2O_2 yields with added

dx.doi.org/10.1021/jp111918v |J. Phys. Chem. C 2011, 115, 8144–8149

Al_2O_3 that are nearly independent of pH in the range of ~4−11. The yields of H_2O_2 increase at pH less than 4 or greater than 11 in the heavy ion radiolysis of aerated Al_2O_3 slurries. Scavenger capacity studies in gamma radiolysis using methanol as an $OH^•$ radical scavenger show that the decrease in H_2O_2 yields with added Al_2O_3 occurs at relatively long time scales and is probably due to reaction of the solid nanoparticles with $OH^•$ radicals. Increasing the scavenging capacity up to about 10^{10} s^{-1} for the hydrated electron using NO_3^- leads to an increase in H_2O_2 yields in aqueous solutions with and without added Al_2O_3. At even higher scavenging capacities the results with added Al_2O_3 are very different than in aqueous solutions alone. The addition of Al_2O_3 can possible inhibit scavenging of the precursor to the $OH^•$ radical by NO_3^-, or more likely, the Al_2O_3 reacts with a secondary product formed in high concentration NO_3^- solutions.

■ ACKNOWLEDGMENT

The authors thank Prof. Michael Wiescher for making the facilities of the Notre Dame Nuclear Science Laboratory available to us. The Nuclear Science Laboratory is supported by the U.S. National Science Foundation. The Notre Dame Radiation Laboratory is supported by the Office of Basic Energy Sciences of the U.S. Department of Energy. This contribution is NDRL-4871 from the Notre Dame Radiation Laboratory.

■ REFERENCES

(1) Pastina, B.; LaVerne, J. A. *J. Phys. Chem. A* **1999**, *103*, 1592.
(2) Jonsson, M.; Nielson, F.; Roth, O.; Ekeroth, E.; Nilsson, S.; Hossain, M. *Environ. Sci. Technol.* **2007**, *41*, 7087.
(3) Petrik, N. G.; Alexandrov, A. B.; Vall, A. I. *J. Phys. Chem. B* **2001**, *105*, 5935.
(4) LaVerne, J. A.; Tandon, L. *J. Phys. Chem. B* **2002**, *106*, 380.
(5) Hiroki, A.; Pimblott, S. M.; LaVerne, J. A. *J. Phys. Chem. A* **2002**, *106*, 9352.
(6) Buxton, G. V. The Radiation Chemistry of Liquid Water: Principles and Applications. In *Charged Particle and Photon Interactions with Matter*; Mozumder, A., Hatano, Y., Eds.; Marcel Dekker: New York, 2004; p 331.
(7) Pastina, B.; LaVerne, J. A. *J. Phys. Chem. A* **2001**, *105*, 9316.
(8) Elliot, A. J.; McCracken, D. R. *Fusion Eng. Des.* **1990**, *13*, 21.
(9) Kitajima, N.; Fukuzumi, S.; Ono, Y. *J. Phys. Chem.* **1978**, *82*, 1505.
(10) Ono, Y.; Matsumura, T.; Kitajima, N.; Fukuzumi, S. *J. Phys. Chem.* **1977**, *81*, 1307.
(11) Klissurski, D.; Hadjiivanov, K.; Kantcheva, M.; Gyurova, L. *J. Chem. Soc., Faraday Trans.* **1990**, *86*, 385.
(12) Amorelli, A.; Evans, J. C.; Rowlands, C. C. *J. Chem. Soc., Faraday Trans. I* **1988**, *84*, 1723.
(13) Anpo, M.; Che, M.; Garrone, E.; Giamello, E.; Paganini, M. C. *Top. Catal.* **1999**, *8*, 189.
(14) Giamello, E.; Fubini, B.; Volante, M.; Costa, D. *Colloids Surf.* **1990**, *45*, 155.
(15) Giamello, E.; Calosso, L.; Fubini, B.; Geobaldo, F. *J. Phys. Chem.* **1993**, *97*, 5735.
(16) Murphy, D. M.; Griffiths, E. W.; Rowlands, C. C.; Hancock, F. E.; Giamello, E. *Chem. Commun.* **1997**, 2177.
(17) Kolobneva, L. I. *Met. Sci. Heat Treat.* **2004**, *46*, 474.
(18) Ziegler, J. F.; Biersack, J. P.; Littmark, U. *The Stopping and Range of Ions in Solids*; Pergamon: New York, 1985.
(19) Ghormley, J. A.; Stewart, A. C. *J. Am. Chem. Soc.* **1956**, *78*, 2934.
(20) Hochanadel, C. J. *J. Phys. Chem.* **1952**, *56*, 587.
(21) Roth, O.; LaVerne, J. A. *J. Phys. Chem. A* **2011**, *115*, 700.
(22) LaVerne, J. A. Radiation Chemical Effects of Heavy Ions. In *Charged Particle and Photon Interactions with Matter*; Mozumder, A., Hatano, Y., Eds.; Marcel Dekker, Inc: New York, 2004; p 403.
(23) Appleby, A; Schwarz, H. A. *J. Phys. Chem.* **1969**, *73*, 1937.
(24) Buxton, G. V.; Greenstock, C. L.; Helman, W. P.; Ross, A. B. *J. Phys. Chem. Ref. Data* **1988**, *17*, 513.
(25) Fenton, H. T. H. *J. Chem. Soc. Proc.* **1893**, *9*, 113.
(26) Wardman, P.; Candeias, L. P. *Radiat. Res.* **1996**, *145*, 523.
(27) Hiroki, A.; LaVerne, J. A. *J. Phys. Chem. B* **2005**, *109*, 3364.
(28) Lousada, C. M.; Jonsson, M. *J. Phys. Chem. C* **2010**, *114*, 11202.
(29) Frumkin, A.; Obrutshewa, A. *Nature* **1926**, *117*, 790.
(30) Wright, W. M.; Rideal, E. K. *Trans. Faraday Soc.* **1928**, *24*, 530.
(31) Schreier, M.; Feltes, T. E.; Schaal, M. T.; Regalbuto, J. R. *J. Colloid Interface Sci.* **2010**, *348*, 571.